Leakage current mechanisms in lead-based thin-film ferroelectric capacitors

B. Nagaraj, S. Aggarwal, T. K. Song, T. Sawhney, and R. Ramesh
Department of Materials and Nuclear Engineering, University of Maryland, College Park, Maryland 20742
(Received 29 June 1998; revised manuscript received 26 January 1999)

Current-voltage (I-V) behaviors of $Pb(Zr, Ti)O_3$-based capacitors with $(La, Sr)CoO_3$ electrodes were studied to investigate the dominant leakage mechanism. Epitaxial $(La,Sr)CoO_3/Pb(Zr,Ti)O_3/(La,Sr)CoO_3$ capacitors were fabricated to simplify the analysis and eliminate any effects of granularity. The I-V characteristics were almost symmetric and temperature dependent with a positive temperature coefficient. The leakage current at low fields (<0.5 V or 10 kV/cm) shows Ohmic behavior with a slope of nearly 1 and is nonlinear at higher voltages and temperatures. Further analysis suggests that at higher fields and temperatures, bulk-limited field-enhanced thermal ionization of trapped carriers (i.e., Poole-Frenkel emission) is the controlling mechanism. The activation energies calculated for the films are in the range 0.5–0.6 eV. These energies are compatible with Ti^{4+} ion acting as the Poole-Frenkel centers. [S0163-1829(99)01124-8]

INTRODUCTION

Ferroelectric thin films are well recognized as capacitor materials in nonvolatile and dynamic random access memory (RAM) applications. Leakage current through thin dielectric films is usually unavoidable and its magnitude and mechanism depend on the material parameters, fabrication procedure, and testing conditions. Unlike in dynamic RAM's, leakage current is not of serious concern in nonvolatile RAM's, though a low leakage current is still one of the desirable qualities. This is because leakage currents can impact the long-term reliability of storage elements. However, leakage currents can also be used as a scientific tool to understand the basic properties of the capacitor. A systematic study of the mechanism of conduction can provide a wealth of information regarding interface and bulk space charge. This knowledge in turn can be invaluable in understanding device-related reliability issues such as imprint, fatigue, polarization relaxation, resistance degradation, and breakdown. Fatigue is the loss of polarization due to bipolar cycling of the capacitor, and imprint is the preference of a ferroelectric capacitor for one polarization state.[1] There is limited understanding of fatigue in $Pt/Pb(Zr,Ti)O_3/Pt$ (Pt/PZT/Pt) heterostructures, with considerable disagreement regarding the degradation mechanism. For example, fatigue has been attributed to domain pinning[2] or space charge.[3] However, when Pt electrodes are replaced by oxide electrodes such as RuO_2, $SrRuO_3$ and $(La,Sr)CoO_3$ (LSCO), the capacitors show excellent fatigue and imprint properties.[4,5] It has been proposed that oxide electrodes act as sinks for oxygen vacancies, thereby eliminating fatigue. Unfortunately, there is no rigorous understanding of the differences in the Pt/PZT and LSCO/PZT interfaces. We believe these interfaces are responsible for the observed differences in the behavior of the capacitors. This study is part of an effort undertaken to rigorously understand the LSCO/PZT interface with an end goal of correlating the leakage current mechanism(s) to the degradation mechanisms of LSCO/PZT/LSCO capacitors.

The correlation between trap states and electrical properties has been extensively studied in SiO_2, which is a traditional dielectric material.[6–11] In contrast, there are very few unambiguous and quantitative studies on ferroelectric thin films addressing this issue. There are several studies of leakage in perovskite-type titanate thin films including $(Ba,Sr)TiO_3$, $SrTiO_3$ and $Pb(Zr, Ti)O_3$ thin films.[12–21] Studies on Pt/PZT/Pt structures reported Schottky emission with a barrier potential of 1.41 eV.[22–24] There are very few studies on the oxide-electrode/PZT interface, which comprehensively address leakage current mechanisms in such capacitors. Since, it is most likely that oxide electrodes will be used to contact PZT-based ferroelectric capacitors, it is imperative that an exhaustive understanding be developed. Such an understanding would also enable one to model and predict the behavior of these interfaces. In this paper, we report on the leakage current mechanism(s) in LSCO/PZT/LSCO capacitors. The correlation between the degradation of ferroelectric capacitors and their leakage current mechanisms will be discussed in future publications.

DEFECT CHEMISTRY

In order to develop a comprehensive understanding of the LSCO/PZT interface one needs to consider the point defects in the two materials, LSCO and PZT. Both materials have perovskite-type structures, and are built around an oxygen octahedron. As such they can be expected to have similar types of defects. For example, interstitial cationic defects are known not to exist in these types of structures, as demonstrated in earlier studies.[25] Therefore only oxygen vacancies and cation vacancies need to be considered. An oxygen vacancy will ionize to give two electrons as follows:[26,27]

$$(O^{2-}{}_{O^{2-}})^{x} = \tfrac{1}{2}O_2 + (V_{O^{2-}})^{\bullet\bullet} + 2e'. \tag{1}$$

The above reaction uses the Kröger-Vink notation,[28] wherein the structural element is represented as $(S_P)^c$, where S is the species, P is the crystallographic position and c is the charge; x is for neutral, the prime implies a negative charge, and $\bullet$ implies a positive charge. Since, LSCO and PZT are both p-type materials, i.e., holes are the majority electronic carriers, the electrons can recombine with the holes, i.e., $nil = e' + h^{\bullet}$. To summarize, oxygen vacancies decrease the number of holes as follows, as is observed in these systems:

$$2h^{\bullet} + (O^{2-}{}_{O^{2-}})^{x} = \tfrac{1}{2}O_2 + (V_{O^{2-}})^{\bullet\bullet}. \quad (2)$$

Furthermore in PZT there are lead and oxygen vacancies due to PbO volatility, created via the Schottky reaction[29,30]

$$(Pb^{2+}{}_{Pb^{2+}})^{x} + [(O^{2-}{}_{O^{2-}})^{x}] = (V_{Pb^{2+}})'' + [(V_{O^{2-}})^{\bullet\bullet}] + PbO. \quad (3)$$

Also, Pb^{2+} ions can oxidize to Pb^{3+}, thereby creating a lead site vacancy for every two oxidized Pb ions, as shown below:[31]

$$3(Pb^{2+}{}_{Pb^{2+}})^{x} + O_2 = (V_{Pb^{2+}})'' + 2(Pb^{3+}{}_{Pb^{2+}})^{\bullet} + 2PbO. \quad (4)$$

The oxidized Pb^{3+} ions are singly positively charged holes compared with the neutral lattice. These mobile holes would lead to a lowering of the electrical resistivity of the film and to poor ferroelectric performance of the devices. Finally, some of the Ti^{4+} ions can be present in the Ti^{3+} state due to oxygen loss, shown as

$$2(Ti^{4+}{}_{Ti^{4+}})^{x} + [(O^{2-}{}_{O^{2-}})^{x}] = 2(Ti^{3+}{}_{Ti^{4+}})' + [(V_{O^{2-}})^{\bullet\bullet}] + \tfrac{1}{2}O_2. \quad (5)$$

All these defects need to be considered when analyzing the interfacial and transport behavior of these materials, and are considered in our analysis of the current-voltage mechanisms. Furthermore, in polycrystalline materials, grain boundaries can increase defect concentrations, as demonstrated in other materials.[32] In PZT films this may give rise to a distribution of energy states throughout its band gap, thus altering the band structure. To simplify our analysis and eliminate any granularity effects, we worked with epitaxial ferroelectric capacitors in this study.

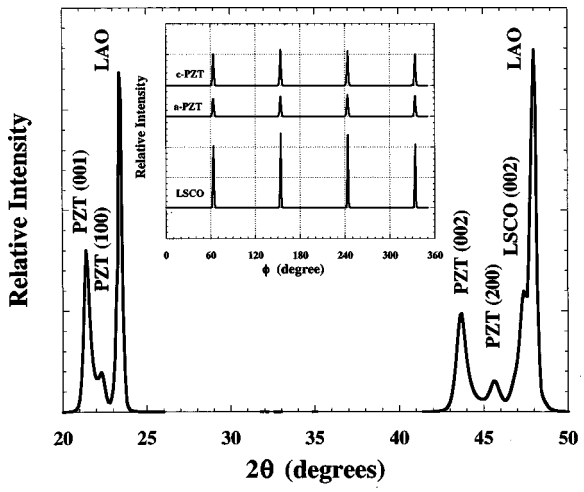

FIG. 1. X-ray-diffraction pattern for LSCO/PZT (300 nm)/LSCO heterostructures. Inset shows ϕ scans for LSCO and PZT showing in-plane orientational symmetry.

EXPERIMENTS

PZT capacitors with LSCO electrodes were fabricated to investigate the leakage current mechanism. Epitaxial $PbZr_{0.2}Ti_{0.8}O_3$ thin-film capacitors with $La_{0.5}Sr_{0.5}CoO_3$ electrodes were grown at a temperature of 650 °C on (001) $LaAlO_3$ substrates by pulsed laser ablation. The thin-film capacitor stacks were grown in an oxygen pressure of 100 m Torr, and after deposition cooled in 760-Torr oxygen. The thickness of the PZT films was varied between 1200 to 3600 Å (in steps of 600 Å), and the thickness of the LSCO electrodes was fixed at 1000 Å. To investigate the effect of dopants, epitaxial $Pb_{0.9}La_{0.1}Zr_{0.2}Ti_{0.8}O_3$ ($\sim$2000 Å) capacitors with LSCO electrodes were also fabricated. The phase purity of each of the stacks was confirmed by using x-ray diffraction. Figure 1 shows the x-ray-diffraction spectrum for a 300-nm PZT film with LSCO electrodes. Note that strong

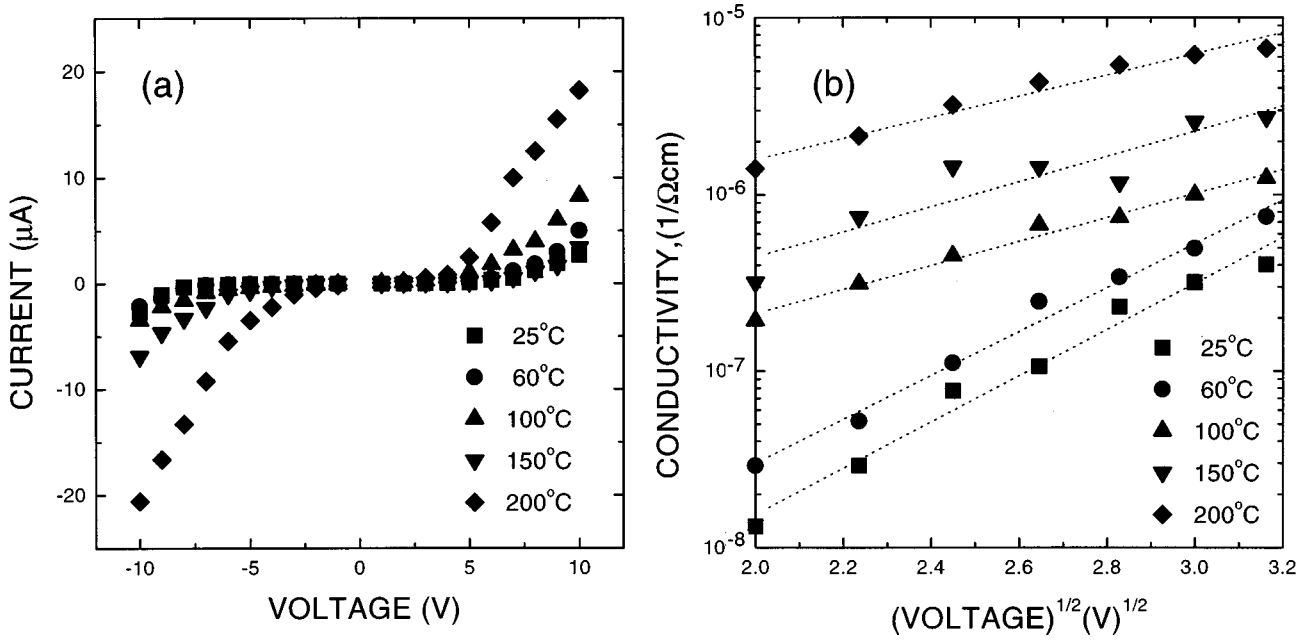

FIG. 2. (a) I-V-T plots for a typical LSCO/PZT/LSCO capacitor showing nonlinear I-V characteristics and a positive temperature coefficient of the current. (b) σ-$V^{1/2}$-T plot (σ plotted on logarithmic scale) for a typical LSCO/PZT/LSCO capacitor showing linear trend at fields higher than 10^5 V/cm.

(00l) reflections for LSCO and PZT are observed, along with smaller (100) reflections of PZT corresponding to a minor fraction of a-axis domains. The inset shows the ϕ scans for the LSCO and PZT (101) reflection. The four peaks separated by 90° indicate locking of in-plane orientational symmetry and cube on cube growth of the film. For electrical measurements, test capacitors with Pt dots of 50-μm diameter on the LSCO top electrodes were delineated by a photolithographic lift-off process, followed by etching the uncovered top LSCO layer by nitric acid. Contact to the bottom electrode was achieved by capacitive coupling from a large Pt contact on the wafer.

For all samples, polarization-voltage (P-V) loops were measured using Radiant Technologies pulsed testing system (RT66A). The leakage current through the capacitors were measured using Keithley 617 programmable electrometer over a temperature range of 300–600 K. The ferroelectric capacitor was switched by increasing the applied voltage to ± 10 V before measuring the leakage current from 0 to ± 10 V. This method was adopted to prevent any contributions from switching currents. Further, the steady-state leakage current was measured through a step voltage technique with a hold time of 1 min at each step. At each voltage, an average of five current readings was taken. Thus the transport behavior in these capacitors cannot be attributed to domain processes involving either 90° or 180° domains. 90° domains are believed to be immobile during switching, while the switching of 180° domains leads to a switching transient current of a duration much shorter than the hold time used in this experiment (1 min). Since our measurements are carried out under steady-state conditions, we believe that the currents measured in our experiments are primarily due to the transport of charged species.

RESULTS AND DISCUSSION

A number of conduction mechanisms are possible through thin insulating films depending on the microstructure, temperature, thickness, and interelectrode barrier. More than one mechanism can simultaneously operate, or separate mechanisms can dominate at different conditions of field and temperature. The current-voltage characteristics were nearly symmetric for all capacitors investigated with respect to voltage polarity, as shown in Fig. 2(a). The current densities measured at 2 V and room temperature, for films 0.3-μm thick, were of the order of 10^{-5} A/cm^2. Notice the temperature sensitivity of the conduction, specifically the positive temperature coefficient, in Fig. 2(a). This pronounced temperature dependence and exponential I-V behavior rules out the possibility of tunneling and space charge limited conduction. Further graphical analysis of the data in Fig. 2(a) indicates that the conduction is Ohmic at fields lower than 10 kV/cm, and nonlinear at higher fields. Ohmic behavior has been observed at low fields by other authors as well in (Ba,Sr)TiO_3 SiO_2, and TiO_2 thin films.[14,33–37] However, the behavior is not very clear in the field range between 10^4 and 10^5 V/cm, especially at lower temperatures. Though the $\ln \sigma$-$V^{1/2}$ trend is linear in this range, at about 4 V there is an increase in slope at lower temperatures, while there is a decrease in slope at higher temperatures as shown in Fig. 3. It appears that more than one mechanism is operating in the

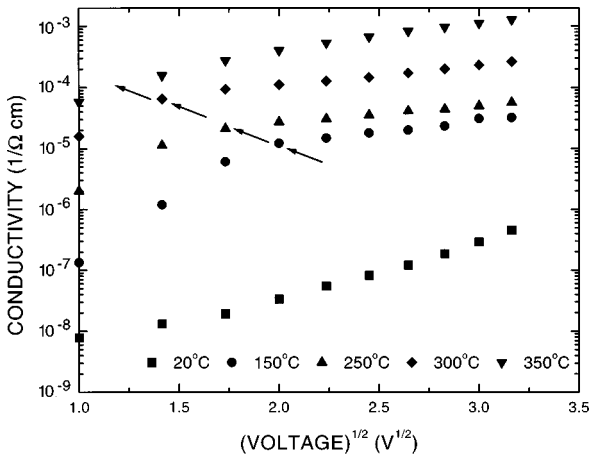

FIG. 3. σ-$V^{1/2}$-T plot for a typical LSCO/PZT/LSCO capacitor at fields higher than 10^4 V/cm.

field range of 10^4–10^5 V/cm. Beyond 10^5 V/cm, a similar trend is observed for all temperatures indicating one dominant leakage mechanism, which we have investigated in this study. In this field range, the $\ln \sigma$-$V^{1/2}$ trend is linear as seen in Fig. 2(b), indicating the possibility of either Schottky or Poole-Frenkel emission.

Current transport in dielectric thin films at high fields and temperatures is usually determined to be interface limited Schottky emission or bulk-limited Poole-Frenkel emission.[11–15,34] Schottky emission is very similar to thermionic emission from the metal surface into the vacuum, with the following difference. In the case of Schottky emission, the carriers are emitted from the electrode surface into the conduction band of the semiconductor, aided by the barrier lowering produced by the combined effect of the image force interaction and the applied field. The current-voltage relationship for the Schottky emission is given by[38]

$$J = A^* T^2 \exp -(\Phi - \beta_S V^{1/2})/kT, \tag{6}$$

where $\beta_s = (q^3/4\pi\varepsilon_0 K d)^{1/2}$. A^* is the modified Richardson-Dushman constant, Φ is the interfacial barrier height and $\beta_s V^{1/2}$ is the lowering of the barrier height due to the image force interaction and the applied field. Poole-Frenkel (PF) emission is the field-assisted thermal ionization of trapped carriers into the conduction band of the insulator, and the PF conductivity is given by[39]

$$\sigma = c \exp -(E_I - \beta_{\mathrm{PF}} V^{1/2})/kT \quad \text{where} \quad \beta_{\mathrm{PF}} = (q^3/\pi\varepsilon_0 K d)^{1/2} \tag{7}$$

and

$$\sigma_0 = c \exp(-E_I/kT). \tag{8}$$

E_I is the trap ionization energy, and $\beta_{\mathrm{PF}} V^{1/2}$ is the barrier lowering due to applied field. It can be seen that their functional relationships are similar but with one key difference. The barrier lowering coefficient β_{PF} in the case of Poole-Frenkel emission is twice that of the Schottky-barrier lowering coefficient β_s. This is because of the fact that the distance between the escaping electron and the trap site, in the case of PF emission, is half that between the escaping electron and the image charge, in the case of Schottky emission.

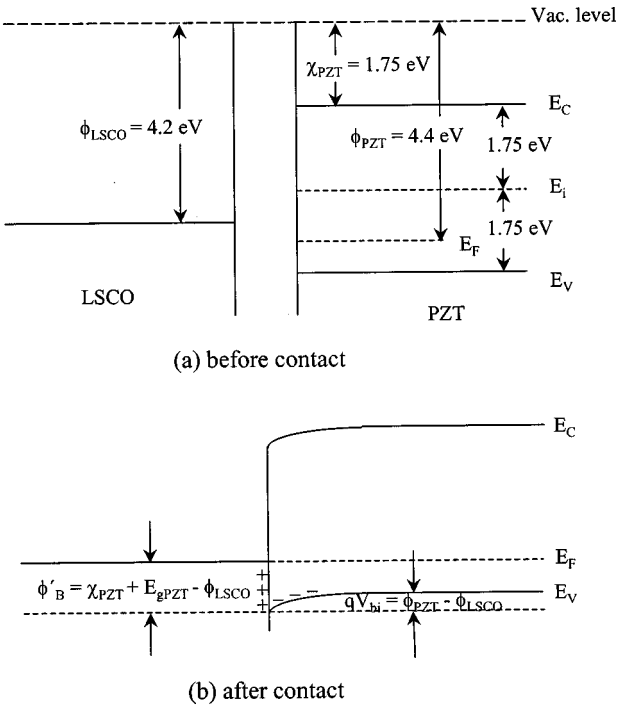

FIG. 4. Band diagram of LSCO/PZT (*p* type) assuming an ideal interface.

Prior to analyzing the experimental data for the type of emission, we examined the possibility of formation of a Schottky barrier, considering a simple band diagram of the material systems used in this investigation. A Schottky barrier is possible with an *n*-type semiconductor, if the work function of metal Φ_m is greater than the work function of semiconductor Φ_{sc} while it is reverse for a *p*-type semiconductor ($\Phi_{sc} > \Phi_m$). The work function of LSCO is 4.6 eV.[40] The work function of undoped PZT, Φ_{PZT} is 3.5 eV,[41] and the band gap of PZT is about 3.5 eV.[42] If one treats PZT as a wide-band-gap semiconductor, then depending on the nature of PZT (viz. *p* or *n* type), a Schottky barrier may or may not be formed. These scenarios are discussed below.

Undoped PZT is reported to exhibit *p*-type conductivity, which is attributed to lead vacancies in the PZT unit cell.[43] There is some scatter in the work-function data for PZT (2.6–4.4 eV) and for LSCO [4.2 eV (Ref. 5) to 4.6 eV (Ref. 40)] reported in the literature. If one believes the work function for PZT to be 2.6 eV (Ref. 31) or 3.5 eV, which are less than that of LSCO (4.6 eV), holes can flow from LSCO to PZT, leading to accumulation, i.e., no Schottky barrier will be formed. If the work function for PZT is larger than 4.6 eV, then a depletion layer will be formed. Figure 4 shows energy-band diagrams of *p*-type PZT with a work function of 4.4 eV, and LSCO with a work function of 4.2 eV before and after contact. As such, holes would flow from PZT to LSCO, and a depletion layer is formed at the interface that rectifies holes [Fig. 4(b)]. The same argument would hold true for Pt electrodes (ϕ_{Pt}=5.3 eV) with PZT (when considering electron exchange) and as such one would not expect a Schottky barrier. We note that several investigators have attributed the *I-V* characteristics of Pt/PZT/Pt to a Schottky-type contact. Therefore it would be premature to disregard the possibility of Schottky contact in the LSCO/PZT/LSCO case at this stage.

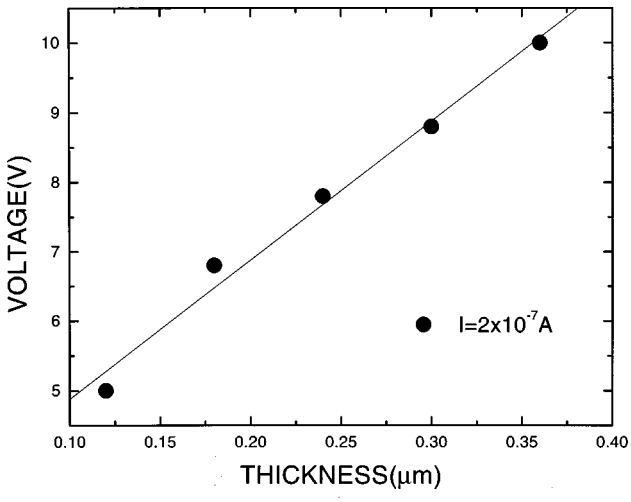

FIG. 5. *V-d* plot for a current of 1×10^{-7} Å in LSCO/PZT/LSCO capacitor showing a linear trend indicating a uniform field in the bulk of PZT.

The second possibility is that, during the top electrode deposition, oxygen vacancies accumulate near the interface making it an *n*-type region, in which case a Schottky barrier of height equal to the difference between the work functions of LSCO, and *n*-type PZT will be formed. This is how one can explain the additional formation of a Schottky barrier in Pt/PZT/Pt capacitors. However, irrespective of the type of PZT near the interface, any interface states present, depending on the magnitude and nature, can have a deciding role on the barrier formation.

In case there are ionized oxygen vacancies formed at the interface, there will be free electrons making the interface *n* type [see the defect chemistry equation (1)], which could then lead to a Schottky-type contact. Therefore, to investigate further the possibility of a Schottky-type contact, the experimental data were analyzed as explained below. The distinction between Schottky and Poole-Frenkel emission is based on whether the effect is electrode or bulk dominated, along with the respective activation energies that can be related to the difference in work function between the electrode material and the dielectric or possible traps in the dielectric. The high-frequency dielectric constant obtained from the slope of Schottky or Poole-Frenkel plots can also indicate the possible mechanism.[14] Though the current-voltage data gave a linear fit to both Schottky and PF plots, the right order of the high-frequency dielectric constant of about 7 was obtained for all the films studied only from PF slopes. The high-frequency dielectric constant (n^2) of (Pb,La)TiO_3 and $BaTiO_3$ films at $\lambda = 0.4\,\mu$m is about 6.5.[44] Assuming PZT to have a similar value, the experimentally obtained value of about 7 indicates that the observed conduction mechanism is Poole-Frenkel emission.

The *I-V* measurements for PZT films of various thicknesses show a linear voltage-thickness dependence for a certain current as shown in Fig. 5. This indicates that the field strength is uniform throughout the film, and that the current depends on voltage and film thickness only through the electric field. Further, the voltage at which the linear trend in $\ln\sigma$-$V^{1/2}$ plot starts reduces as the temperature is increased, as can be seen in Fig. 3. These observations verify that the

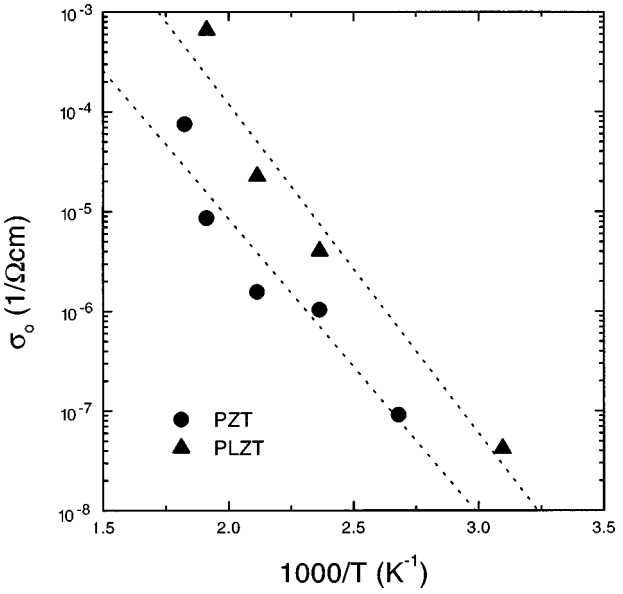

FIG. 6. σ_0-$1/T$ plots for PZT and PLZT capacitors with LSCO electrodes.

emission is field and temperature activated, which are the characteristics of Poole-Frenkel emission.

The ionization energy of the traps obtained from the slope of $\ln \sigma_0$-$1/T$ plots (Fig. 6) are in the range of 0.5–0.6 eV for PZT and (Pb,La)$ZrTiO_3$ capacitors. Note that the trap ionization energy in both ferroelectric films is similar, suggesting that the trap center is common to them. This implies that La doping does not influence the leakage mechanism in PZT-based capacitors. Though not shown here, Nb doping also does not influence the trap activation energy. In PZT, there are two cations that can change valence states: Pb and Ti. The ionization energy for Pb ions [see Eq. (3)][31] is ~0.26 eV, which implies that Pb ions do not act as Poole-Frenkel centers in the high-temperature, high-field region. The ionization energy of Ti^{4+} to Ti^{3+} is estimated to be ~0.5 eV for PZT.[45] This indicates that Ti ions act as Poole-Frenkel centers, and give rise to PF emission as follows [see Eq. (4)]:

$$Ti^{4+} = Ti^{3+} + h^{\bullet}. \tag{9}$$

The released holes give rise to PF conduction.

SUMMARY

The study of the leakage current mechanism through PZT and PLZT capacitors shows that the conduction is Ohmic at low fields. At higher fields and temperatures, *I-V* plots are nonlinear and nearly symmetric. The $\ln \sigma$-$V^{1/2}$ plots at high temperatures and fields are linear, their slope yielding a value of 7 for the dielectric constant of PZT and PLZT films. This indicates that the mechanism of conduction could be the bulk-limited Poole-Frenkel emission at high fields and temperatures. The fact that the electric field is uniform in the ferroelectric film and that both temperature and field activate the current further confirms the mechanism to be Poole-Frenkel emission. The trap ionization energies calculated from the slope of $\ln \sigma_0$-$1/T$ plots, are in the range 0.5–0.6 eV for PZT and PLZT capacitors. This suggests that the same trap center acts as the Poole-Frenkel center in both PZT and PLZT films. The fact that the ionization energy of Ti^{4+} to Ti^{3+} is ~0.5 eV suggests that Ti^{4+} could be the possible PF center. The absence of a space-charge region at the interface could be the reason for good fatigue and imprint characteristics in these capacitors.

ACKNOWLEDGMENTS

This work was supported by NSF-MRSEC Grant No. DMR96-32521 and by the Center for Superconductivity Research.

[1] J. F. Scott and C. A. Paz de Araujo, Science **246**, 1400 (1989).
[2] D. Dimos, W. L. Warren, H. N. Al-Shareef, and B. A. Tuttle, J. Appl. Phys. **80**, 1682 (1996).
[3] S. B. Desu, Phys. Status Solidi A **151**, 467 (1995).
[4] R. Ramesh and V. G. Keramidas, Annu. Rev. Mater. Sci. **25**, 647 (1995).
[5] S. Sadhashivan, S. Aggarwal, T. K. Song, R. Ramesh, J. T. Evans, Jr., B. A. Tuttle, W. L. Warren, and D. Dimos, J. Appl. Phys. **83**, 2165 (1998).
[6] J. M. Benedetto, H. E. Boesch, F. B. Mclean, and J. P. Mize, IEEE Trans. Nucl. Sci. **NS-32**, 3916 (1985).
[7] T. R. Oldham, A. J. Lelis, and F. B. Mclean, IEEE Trans. Nucl. Sci. **NS-33**, 1203 (1986).
[8] D. J. Dumin and J. Maddux, IEEE Trans. Electron Devices **ED-40**, 986 (1993).
[9] R. S. Scott, R. Subramonium, and D. J. Dumin, J. Electrochem. Soc. **142**, 930 (1995).
[10] D. J. Dumin, J. R. Maddux, R. S. Scott, and R. Subramonium, IEEE Trans. Electron Devices **ED-41**, 1570 (1994).
[11] H. Hirose and Y. Wada, Jpn. J. Appl. Phys. **4**, 636 (1965).
[12] K. Abe and S. Komatsu, Jpn. J. Appl. Phys. **31**, 2985 (1992).
[13] T. Kuroiwa, T. Honda, H. Watarai, and K. Sato, Jpn. J. Appl. Phys. **31**, 3025 (1992).
[14] Y. Shimada, Y. Inone, T. Nasu, K. Arita, Y. Nagano, A. Matsuda, Y. Uemoto, E. Fujii, M. Azuma, Y. Oishi, S. Hayashi, and T. Otsuki, Jpn. J. Appl. Phys. **35**, 140 (1996).
[15] K. Numata, Y. Fukuda, K. Aoki, A. Nishimura, Jpn. J. Appl. Phys. **34**, 5245 (1995).
[16] J. F. Scott, C. A. Araujo, B. M. Melnick, L. D. McMillan, and R. Zuleeg, J. Appl. Phys. **70**, 382 (1991).
[17] C. S. Hwang, S. O. Park, C. S. Kang, H.-J. Cho, H.-K. Kang, and S. T. Ahn, Jpn. J. Appl. Phys. **34**, 5178 (1995).
[18] M. Kiyotoshi and K. Eguchi, Appl. Phys. Lett. **67**, 2468 (1995).
[19] R. Waser, in *Science and Technology of Electroceramic Thin Films*, Vol. 284 of *NATO Advanced Study Institutes*, edited by O. Auceillo and R. Waser (Kluwer, London, 1995), p. 223.
[20] S. Dey, J. J. Lee, and P. Alluri, Jpn. J. Appl. Phys. **34**, 3142 (1995).
[21] G. W. Dietz, M. Schumacher, R. Waser, S. K. Streiffer, C. Basceri, and A. I. Kingon, J. Appl. Phys. **82**, 2359 (1997).
[22] H.-M. Chen, J.-M. Lan, J.-L. Chen, and J. Y. Lee, Appl. Phys. Lett. **69**, 1713 (1996).

[23] X. Chen, A. I. Kingon, H. Al-Shreef, and K. R. Bellur, Ferroelectrics **151**, 133 (1994).
[24] H. D. Bhatt, S. B. Desu, D. P. Vijay, Y. S. Hwang, X. Zhang, M. Nagata, and A. Grill, Appl. Phys. Lett. **71**, 719 (1997).
[25] G. V. Lewis and C. R. A. Catlow, Radiat. Eff. **73**, 307 (1983).
[26] S. Madhukar, S. Aggarwal, A. M. Dhote, R. Ramesh, A. Krishnar, D. Keeble, and E. Poindexter, J. Appl. Phys. **81**, 3543 (1997).
[27] M. V. Raymond and D. M. Smyth, Integr. Ferroelectr. **4**, 145 (1994).
[28] F. A. Kröger and H. J. Vink, in *Solid State Physics—Advances in Research and Applications*, edited by F. Seitz and T. Turnbull (Academic, New York, 1957), Vol. 3, pp. 307–435.
[29] R. L. Holman and R. M. Fulrath, J. Appl. Phys. **44**, 5227 (1973).
[30] S. Fushimi and T. Ikeda, J. Am. Ceram. Soc. **50**, 129 (1967).
[31] W. L. Warren, D. M. Smyth, J. Robertson, D. Dimos, C. H. Seager, B. A. Tuttle, and G. E. Pike, (unpublished).
[32] R. Waser and D. M. Smyth, in *Ferroelectric Thin Films: Synthesis and Basic Properties*, edited by C. A. P. Araujo, J. F. Scott, and G. W. Taylor (Gordon and Breach, Singapore, 1996), pp. 47–92.
[33] H. Hirose and Y. Wada, Jpn. J. Appl. Phys. **3**, 179 (1964).
[34] T. E. Hartman, J. G. Blair, and R. Bauer, J. Appl. Phys. **37**, 2468 (1966).
[35] Y. Katsuta, A. E. Hill, A. M. Phahle, and J. H. Calderwood, Thin Solid Films **18**, 53 (1973).
[36] G. M. Rao and S. B. Krupanidhi, J. Appl. Phys. **75**, 2604 (1994).
[37] C. J. Peng, H. Hu, and S. B. Krupanidhi, Appl. Phys. Lett. **63**, 1038 (1993).
[38] M. Ohring, *The Materials Science of Thin Films* (Academic, New York, 1992), pp. 462–472.
[39] J. J. O'Dwyer, *The Theory of Electrical Conduction and Breakdown in Solid Dielectrics* (Clarendon, Oxford, 1973), pp. 236–256.
[40] B. Chalamala, S. Aggarwal, and R. Ramesh (unpublished).
[41] J. A. Bullington, M. D. Ivey, and J. T. Evans, in *Proceedings of the First Symposium on Integrated Ferroelectrics, Colorado Springs* (Gordon and Breach, Chur, Switzerland, 1989), p. 201.
[42] S. E. Bernacki, in *Ferroelectric Thin Films II*, edited by A. I. Kingon, E. R. Myers, and B. Tuttle, MRS Symposia Proceedings No. 243 (Material Research Society, Pittsburgh, 1992), p. 135.
[43] R. Gerson and H. Jaffe, J. Phys. Chem. Solids **24**, 979 (1963).
[44] *Ferroelectrics and Related Substances. Non-Oxides*, edited by K.-H. Hellwege and O. Madelung, Landolt-Bornstein, New Series, Group III, Vol. 28, Pt. b (Springer-Verlag, Berlin, 1991), pp. 232 and 238.
[45] W. L. Warren (private communication).